ATLAS

ATLID Algorithms and Level 2 System Aspects

Algorithm Theoretical Basis Document (ATBD) for Ice product

Code : EC-TN-KNMI-ATL-23
Issue : 1.3
Date : 27/06/11
Authors : S. Berthier
D.P. Donovan
G-J van Zadelhoff

This page intentionally left blank

Issue	Revision	Date	Reason for Change	Author
1.0	Baseline	12/01/11	Version delivered at ESA	S.B., D.D, GJvZ [KNMI]
1.1		26/04/11	Version for the ATLAS final meeting	S.B., D.D, GJvZ [KNMI]
1.2		26/05/11	ATLAS final version	S.B., D.D, GJvZ [KNMI]
1.3		27/06/11	Update after Final Review	S.B., D.D, GJvZ [KNMI]

Table of Contents

1.Purpose and Scope....5
2.Applicable and Reference Documents....6
2.1.Applicable documents....6
2.2.Reference & Related documents....6
2.3.References....6
3. Scientific Background of the algorithm 7
3.1.Algorithm introduction....7
3.2.Physical/mathematical Background....7
3.2.1.Ice/Water discrimination....7
3.2.2.Retrieval Algorithm of IWC....7
3.2.3.Error assessment on the Ice Water Content....8
3.2.4.Retrieval Algorithm of Ice effective radius....8
3.2.5.Error assessment on Ice effective radius....9
Classification of Ice crystal type and associated error....9
4. Justification for the selection of the algorithm....9
5.Mathematical algorithm Description....10
5.1.Input parameters....10
5.2.Configuration parameters....12
5.3.Output parameters....12
5.3.1.Operational output parameters....12
5.4.Algorithm flow charts....13
5.5.Algorithm definition....15
5.5.1.Ice/Water discrimination....15
5.5.2.Retrieval Algorithm of IWC....15
5.5.3.Error assessment on the Ice Water Content....15
5.5.4.Retrieval Algorithm of Ice effective radius....16
5.5.5.Error assessment on Ice effective radius....16
5.5.6.Classification of Ice crystal type and associated error....16
6. Algorithm performance, sensitivity studies, limitations....16
6.1.Comparison with DARDAR-CLOUD product....16
6.2.IWC retrieval : comparison with DARDAR result....17
6.3.Reff retrieval : comparison with DARDAR result....22
7.Validation status....25
8.Future validation needs....25

1. Purpose and Scope

This document describes a procedure for estimating Ice Water Content (IWC) and Effective radius using lidar derived extinction measurements and auxiliary temperature information.

The general flow chart is given in the figure 1. Red boxes give the part of the architecture corresponding to the present module.

This procedure use as an input the extinction at high resolution as processed by the L2a Extinction procedure (A-EBD product).

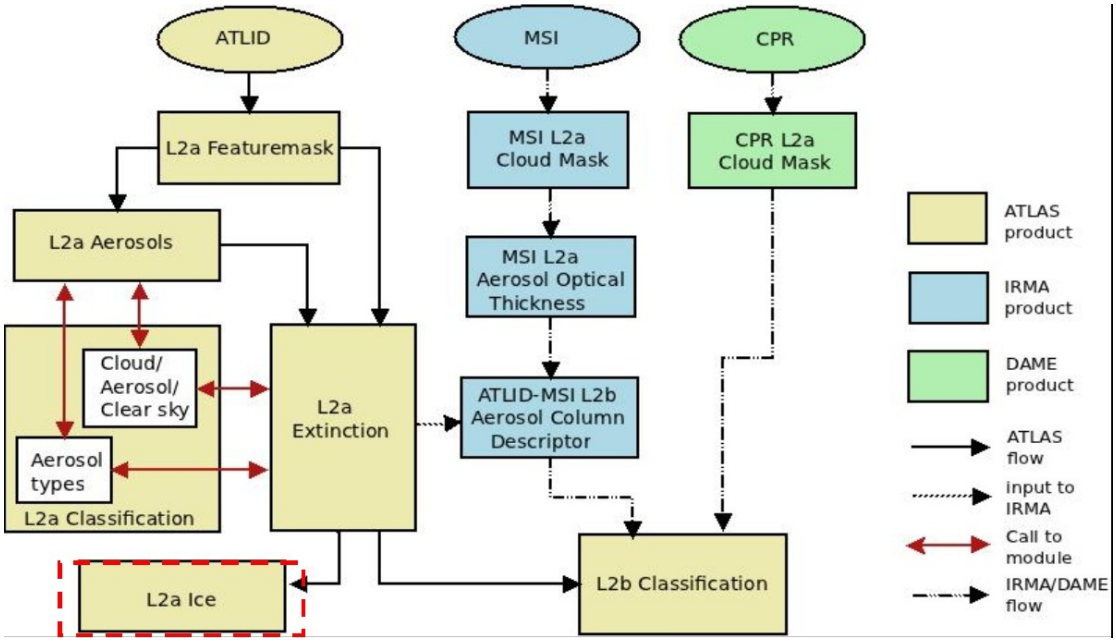

Figure 1: ATLAS General flow chart

2. Applicable and Reference Documents

2.1. Applicable documents

Reference	*Code*	*Title*	*Issue*	*Date*
MRD	ER-RS-ESA-SY-012	EarthCARE Mission Requirements Document	5	11/02/06

2.2. Reference & Related documents

Reference	*Code*	*Title*	*Issue*	*Date*
CASPER-PARD	CASPER-DMS-PARD-001	CASPER Products and Algorithms Requirement Document (PARD)	2.0	10/30/08
CASPER-FINAL	CASPER-DMS-FR-01	CASPER Final Report	1.1	01/30/09
EC-PTR	EC-ICD-ESA-SYS-0314	EarthCARE product table reference	1.3	06/15/10
A-EBD	EC-TN-KNMI-ATL-021	ATLID L2a Extinction, Backscatter & Depolarization	1.2	26-05-11
ATL-FINAL	EC-FR-KNMI-ATL-027	Final report	1	27-05-11

2.3. References

Keyword	Reference
[Heymsfield et al., 2005]	Heymsfield, A. J., D. Winker, and G.-J. van Zadelhoff (2005), Extinction-ice water content-effective radius algorithms for CALIPSO, *Geophys. Res. Lett.*, 32, L10807, doi:10.1029/2005GL022742.
[Foot, 1988]	Foot, J. S. (1988), Some observations of the optical properties of clouds. Part II: Cirrus, Q. J. R. Meteorol. Soc., 114, 145 – 164 .
[Avery, 2010]	Avery, M., D. Winker, M. Vaughan, S. Young, R. Kuehn, Y. Hu, J. Tackett, B. Getzewich, Z. Liu, A. Omar, K. Powell, C. Trepte, and K.-P. Lee, (2010), "A first look at CALIOP/CALIPSO cloud ice water content", submitted to the 25th International Laser and Radar Conference.
[Delanoe et al., 2010]	Delanoë, J., and R. J. Hogan (2010), Combined CloudSat-CALIPSO-MODIS retrievals of the properties of ice clouds, *J. Geophys. Res.*, 115, D00H29, doi:10.1029/2009JD012346.

3. Scientific Background of the algorithm

3.1. Algorithm introduction

The objective of this algorithm is to retrieve, by using the lidar only datasets (backscatter and extinction as retrieved in the L2 datasets), the Ice cloud properties. Using Extinction and temperature parameters, The Ice Water Content (IWC) profiles are retrieved using an existing parametrization given in [Heymsfield et al., 2005]. Using the [Foot, 1988] parametrization and the IWC values previously processed, the effective radius (Reff) profiles can also be assessed.

3.2. Physical/mathematical Background

The effect of clouds on the Earth's atmospheric radiation budget is one of the primary uncertainties in characterizing climate change. Knowledge of IWC and Reff parameters is essential to understand cloud physics and radiative properties. The ATLID lidar is expected to deliver IWC and R_{eff} datasets that will help to reduce this aspect of climate uncertainty. This product is a backup for the L2b lidar+radar cloud products, and a primary product for lidar only cloud products

This algorithm mainly relies upon the parametrization described in [Heymsfield et al, 2005] to estimate IWC and R_{eff}.

3.2.1. Ice/Water discrimination

From the calculation of the depolarization ratio made in the Lidar only version (A-EDB), it is possible to discriminate between Ice and liquid particles. From this discrimination, it is possible to construct the ICE Water Mask (IWM), where ice particles have been identified.

3.2.2. Retrieval Algorithm of IWC

Ice water content (IWC) is reported for all ice clouds retrieved by the lidar only classification. Cloud ice water content is a provisional data product that is calculated as a parametrized function of the Atlid retrieved extinction by ice cloud particles. Adopting an existing power-law relating α and IWC. This relationship was retrieved by Heymsfield. et al. using a combination of in-situ measurements and lidar-radar retrievals, and can be adopted for each individual relevant pixel (k) :

$$IWC(k) = C_0 \left(\frac{\alpha(k)}{1000} \right)^{C_1} . IWM(k) \qquad (1)$$

Where the IWM parameter represent the Ice/Water mask.

Cloud ice amount has been shown to vary with temperature, cloud particle size distribution, and by location inside a cloud. A temperature-dependent parametrization has been considered in [Heymsfield et al., 2005]. This leads to the parameters $C_0 = 89 + 0.62204 . T(^\circ C)$ and $C_1 = 1.02 - 0.00281 . T(^\circ C)$.

These coefficients have been derived from an observed empirical relationship between lidar extinction and an extensive set of in situ measurements of cloud particle properties from numerous field campaigns [Heymsfield et al., 2005]. The relationship between 532 nm extinction and IWC was developed using IWC data between 0-1.0 gm^{-3} with temperatures between -70 and 0 °C. Since, in most, circumstances ice cloud particles are large compared to the lidar wavelengths of 532 and 353 nm it is reasonable to assume that the extinction at 353 nm (the ATLID wavelength) is similar to the extinction at 532 nm so that the parametrization of Heymsfield can be applied to ATLID extinction measurements.

3.2.3. Error assessment on the Ice Water Content

The precision on IWC is linked to one of the extinction retrieval. This last is limited by signal-to-noise ratio, and will varies between night and day and according to the overhead two-way 532 nm transmission.

IWC uncertainty has a range of 0-99.99 gm^{-3}, and is derived directly from the extinction retrieval uncertainty.

The fractional uncertainty of IWC is a simple multiple of the extinction coefficient fractional uncertainty :

$$\sigma_{IWC(k)} = IWC(k) . C_1 . \left(\frac{\sigma_{\alpha(k)}}{\alpha(k)} \right) \qquad (2)$$

3.2.4. Retrieval Algorithm of Ice effective radius

A linear relationship link the Ice effective radius, with the IWC and the extinction α This relation has been produced in [Foot, 1988 ; Heymsfield et al., 2005], for each altitude range k :

$$Re(k) = C . \left(\frac{IWC(k)}{\alpha(k)} \right) . IWM(k) \qquad (3)$$

Where $C = 1.64$, and IWM the Ice/Water mask.

This calculation will be made only where Ice particles as identified inside the ice-water mask (see section 5.5.1.) are present.

3.2.5. Error assessment on Ice effective radius

The fractional uncertainty of the Ice effective radius can be derived from the fractional uncertainties of the IWC and the extinction :

$$\sigma_{Reff(k)} = R_{eff}(k).\sqrt{\left(\frac{\sigma_{IWC(k)}}{IWC(k)}\right)^2 + \left(\frac{\sigma_{\alpha(k)}}{\alpha(k)}\right)^2} \quad (4)$$

Classification of Ice crystal type and associated error

The determination of the Ice crystal type, nor the check for possibility, has not yet been included in the scope of this document.

4. Justification for the selection of the algorithm

According to our knowledge, and by using only the lidar only dataset, the parametrization based approach is the only available method to estimate the IWC. The particular parametrization this algorithm is based on is one of the more comprehensive and up-to-date available in the open literature.

5. Mathematical algorithm Description

5.1. Input parameters

Input is read from the following products :

- The A-EBD (Extinction, Backscatter and Depolarization at High Resolution) product.
- The A-TC (The ATLID Target classification) product.
- The ancillary datasets from ECMWF.

Variable	Symbol	Description	Unit	Dim	Type	Sources	Remarks
Time	**UTC**	UTC time	S	Time	Double	A-EBD	
Latitude	**LAT**	Latitude	Deg.	Time	Real	A-EBD	
Longitude	**LON**	Longitude	Deg.	Time	Real	A-EBD	
Height	**Z**	Height of each radar/lidar gate above mean sea level	m	Time	Real	A-EBD	
Surface_Altitude	$\mathbf{Z_{Alti}}$	Height of surface above mean sea level	m	Time	Real	A-EBD	
ext	**α**	Extinction coefficient	m^{-1}	Time, Height	Real	A-EBD	
D_ext	$\boldsymbol{\sigma_{\alpha}}$	1-sigma-estimated error	m^{-1}	Time, Height	Real	A-EBD	
depol	**δ**	Depolarization ratio	None	Time, Height	Real	A-EBD	
D_depol	$\boldsymbol{\sigma_{\delta}}$	1-sigma-estimated error	None	Time, Height	Real	A-EBD	

Simplified classification	-	liquid/water Simplified classification from A-TC product	None	Time, Height	8-bit unsig nied intege rs	A-TC	0=ground, 1 = clear sky, 2 = liquid cloud, 3 = ice only, 9 = aerosol, 11=stratosphe ric, 13 = don't know, other = NOT USED
L2A-FeatureMask Ancillary datasets from ECMWF							
ECMWF_PRES	**P**	Pressure (ECMWF Field Code 54)	Pa	Heig ht, Time	Real	ECMW F	
ECMWF_T	**T**	Temperatur e (ECMWF Field Code 130)	K	Heig ht, Time	Real	ECMW F	
ECMWF_Hgt	$\mathbf{Z_{ECMWF}}$	Height	m	Heig ht, Time	Real	ECMW F	Along track
ECMWF_Surf_ Alt	$\mathbf{Z_{Surf,EC MWF}}$	Surface Altitude (ECMWF Field Code 010001)	m	Time	Real	ECMW F	Along track

Table 1: Operational input parameters.

5.2. Configuration parameters

Variable	Symbol	Description	Unit	Dim	Type	Source	Remarks
C_1	**C_1**	First Parametrization Coefficient driving the retrieval of IWC	None	None	Real	[Heymsfield et al., 2005] or Algorithm	Configurable
C_2	**C_2**	Second Parametrization Coefficient driving the retrieval of IWC	None	None	Real	[Heymsfield et al., 2005] or Algorithm	Configurable
C	**C**	Parametrization Coefficient driving the retrieval of R_{eff}	None	None	Real	[Foot, 1988] or Algorithm	Configurable

5.3. Output parameters

5.3.1. Operational output parameters

Variable	Symbol	Description	Units	Dim	Type	Destination
1D Coordinate variables						
Time	**UTC**	UTC time	S	Time	Double	Stand Alone Product
Latitude	**LAT**	Latitude	Deg.	Time	Real	Stand Alone Product
Longitude	**LON**	Longitude	Deg.	Time	Real	Stand Alone Product
Height	**Z**	Height above mean sea level	m	Height	Real	Stand Alone Product
Geographic information						
surface_altitude	**Z_{surf}**	Height of surface above mean sea level	m	Time	Real	Stand Alone Product
Ice cloud properties						

Variable	Symbol	Description	Units	Dim	Type	Destination
Mask_Ice	**IWM**	0 = No cloud, 1 = cloud 2= water cloud 3 = ice cloud	None	Time, Height	Integer	Stand Alone Product
Ice_Water_Content	**IWC**	Ice water content	$kg.m^{-3}$	Time, Height	Real	Stand Alone Product
Ice_Effective_Radius	**R_{eff}**	Ice effective radius	m	Time, Height	Real	Stand Alone Product
Errors in the main derived quantities						
ice_ln_water_content_error	**Err_{IWC}**	1-sigma random error in natural logarithm of ice water content	none	Time, Height	Real	Stand Alone Product
ice_ln_effective_radius_error	**Err_{Reff}**	1-sigma random error in natural logarithm of effective radius	none	Time, Height	Real	Stand Alone Product
Type	**None**	Ice crystal type (Plate, Column, ...)	none	Time, Height	Bytes	Stand Alone Product
Quality control variables						
Status	**None**	Retrieval status flag. 0➔ success 1➔ no retrieval attempted (i.e. no ice layer present) 2➔retrieval failed 3➔No data	-	Time	Integer	Stand Alone Product

Table 2: Operational output parameters.

5.4. Algorithm flow charts

The inversion algorithm can be defined by the following sequence of procedures.

Each of these procedures are represented within the flowchart given in Figure 2 by the blocks labelled with Roman numbers.

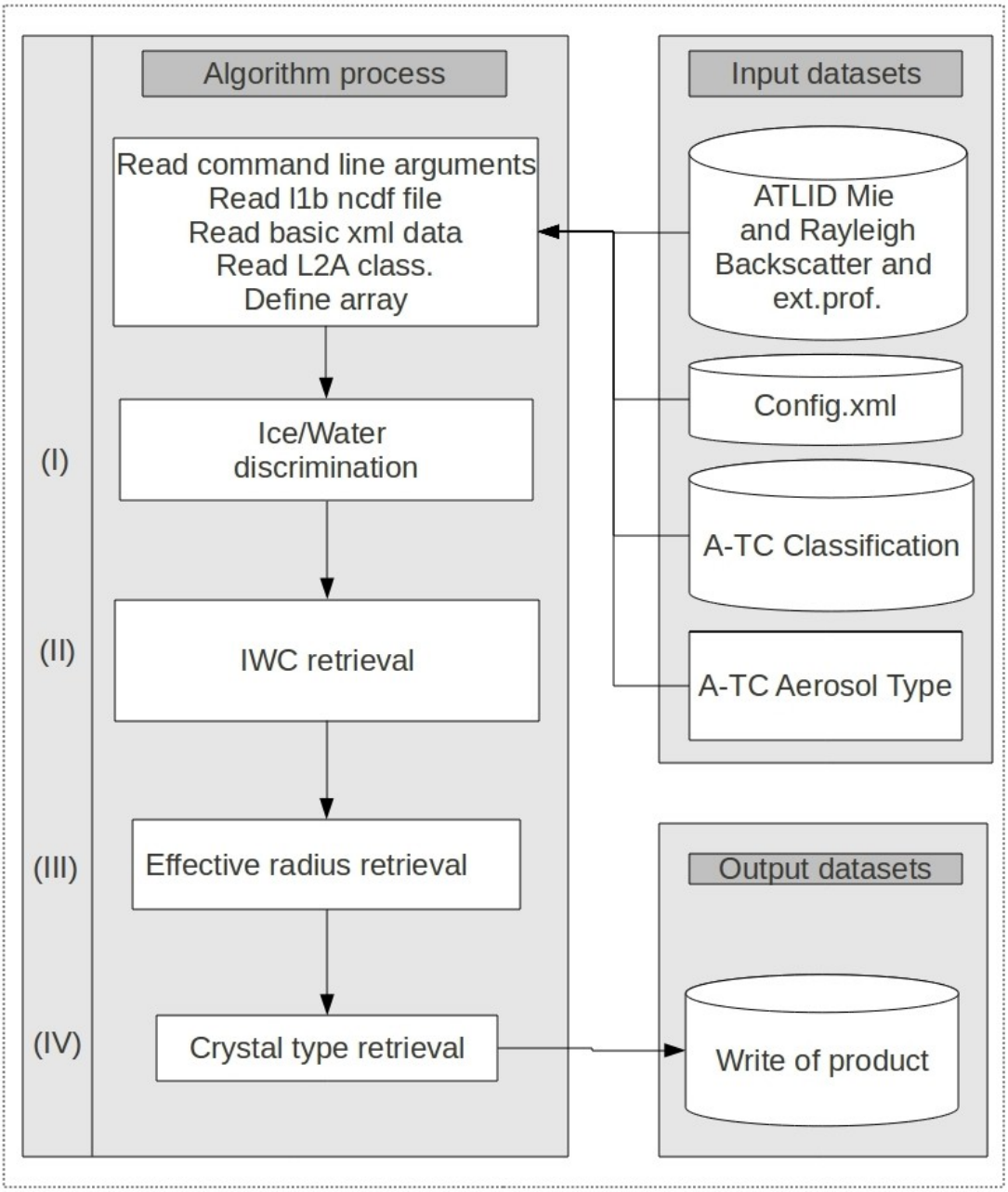

Figure 2: Ice Retrieval Algorithm Flowchart

After that all the datasets has been ingested by the algorithm, through the reading procedure, the four steps can be summarized by :

#	Task	Ref. Section
I	Ice/Water discrimination	Section 5.5.1.
II	IWC assessment	Section 5.5.2.
III	Effective radius retrieval	Section 5.5.4.
IV	Crystal Type retrieval	Section 5.5.6.

Table 3: Algorithm steps and corresponding section in this document.

5.5. Algorithm definition

5.5.1. Ice/Water discrimination

The process of ice-water discrimination is not described further in this document. This procedure is described in detail in a separate document [ATLID Target classification, A-TC ATBD]. From this product, the variable **Simplified classification** is used to localize ice layers. For the purposes of the IWC algorithm, an Ice/Water mask (noted IWM) is constructed, and is defined by setting IWM=1 where the input target mask indicates the presence of ice clouds and 0 otherwise.

5.5.2. Retrieval Algorithm of IWC

The IWC is produced using the simple parametrization :

$$IWC(k) = C_0 \left(\frac{\alpha(k)}{1000} \right)^{C_1} . IWM(k) \qquad (5)$$

Where the IWM parameter represent the Ice/Water mask, and the parameters C_0 and C_1 are respectively equal to $C_0 = 89 + 0.62204 . T(^\circ C)$ and $C_1 = 1.02 - 0.00281 . T(^\circ C)$.

5.5.3. Error assessment on the Ice Water Content

The fractional uncertainty of IWC is a simple multiple of the extinction coefficient fractional uncertainty :

$$\sigma_{IWC(k)} = IWC(k) . C_1 . \left(\frac{\sigma_{\alpha(k)}}{\alpha(k)} \right) \qquad (6)$$

5.5.4. Retrieval Algorithm of Ice effective radius

The effective radius R_{eff} product is produced using the simple parametrization :

$$R_{eff}(k) = C.\left(\frac{IWC(k)}{\alpha(k)}\right).IWM(k) \quad (7)$$

Where $C = 1.64$, k the considered altitude level, and IWM the Ice/Water mask.

5.5.5. Error assessment on Ice effective radius

The error on the effective radius R_{eff} parameter is retrieved by using the following equation :

$$\sigma_{Reff(k)} = R_{eff}(k).\sqrt{\left(\frac{\sigma_{IWC(k)}}{IWC(k)}\right)^2 + \left(\frac{\sigma_{\alpha(k)}}{\alpha(k)}\right)^2} \quad (8)$$

5.5.6. Classification of Ice crystal type and associated error

The determination of the Ice crystal type has not yet been included in the scope of this document.

6. Algorithm performance, sensitivity studies, limitations

6.1. Comparison with DARDAR-CLOUD product

To evaluate the used parametrization the retrieved results are compared to ones that has been retrieved in previous works.

The only existing dataset that can provide this type of information based on space based data is given by the DARDAR-CLOUD product [see Delanoe and Hogan]. This algorithm of Delanoe and Hogan uses a variational method for retrieving profiles of visible extinction coefficient, Ice water content and effective radius in ice cloud using the combination of radar reflectivity, lidar attenuated backscatter and Infrared Radiances in the water-vapour window.

One entire day has been retrieved (8th November 2009) in this study. This amount of data is sufficient to reach a good statistics on the considered parameters (see Table 4 for the size of the dataset, and Figure 3 for the location of the occurrences).

This DARDAR dataset can be separated into three different classes : (1) When only lidar data was available (noted **L**), (2) when only radar data was available (noted **R**), and the last one, (3) when lidar and radar measurements was available (noted **L+R**).

We see by the Table 4 that each class represent roughly one third of the total amount of pixel in the datasets.

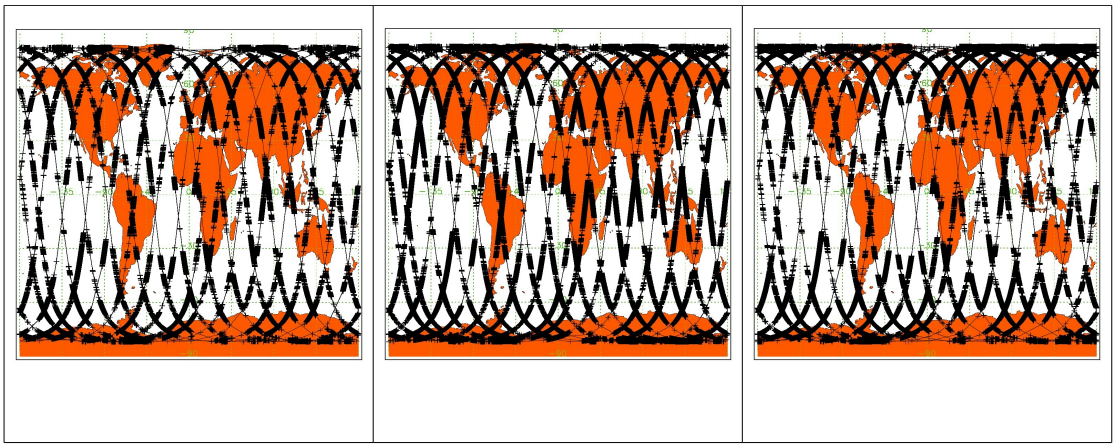

Figure 3: Map of the occurrence of pixels used inside this study : from left to right, (1) the Lidar + Radar pixels, (2) the Lidar pixels, and (3) the Radar pixels.

Lidar + Radar (L+R)	Radar (R)	Lidar (L)	All
4995056 pix	6153504	4807808	15956368
31.31%	38.56%	30.13%	100.00%

Table 4: Amount of ice cloud pixels used in this statistical analysis.

6.2. IWC retrieval : comparison with DARDAR result

Figure 4 depicts the histogram of the extinction as given inside the DARDAR product for, respectively, the L+R and L classes. The extinction corresponding to the **R** classes is not given here, as it is not considered as relevant for our purposes.
From Figure 3, it can be easily noticed the lidar only classes seem to contain more lower extinction value than in the case of the L+R classes.

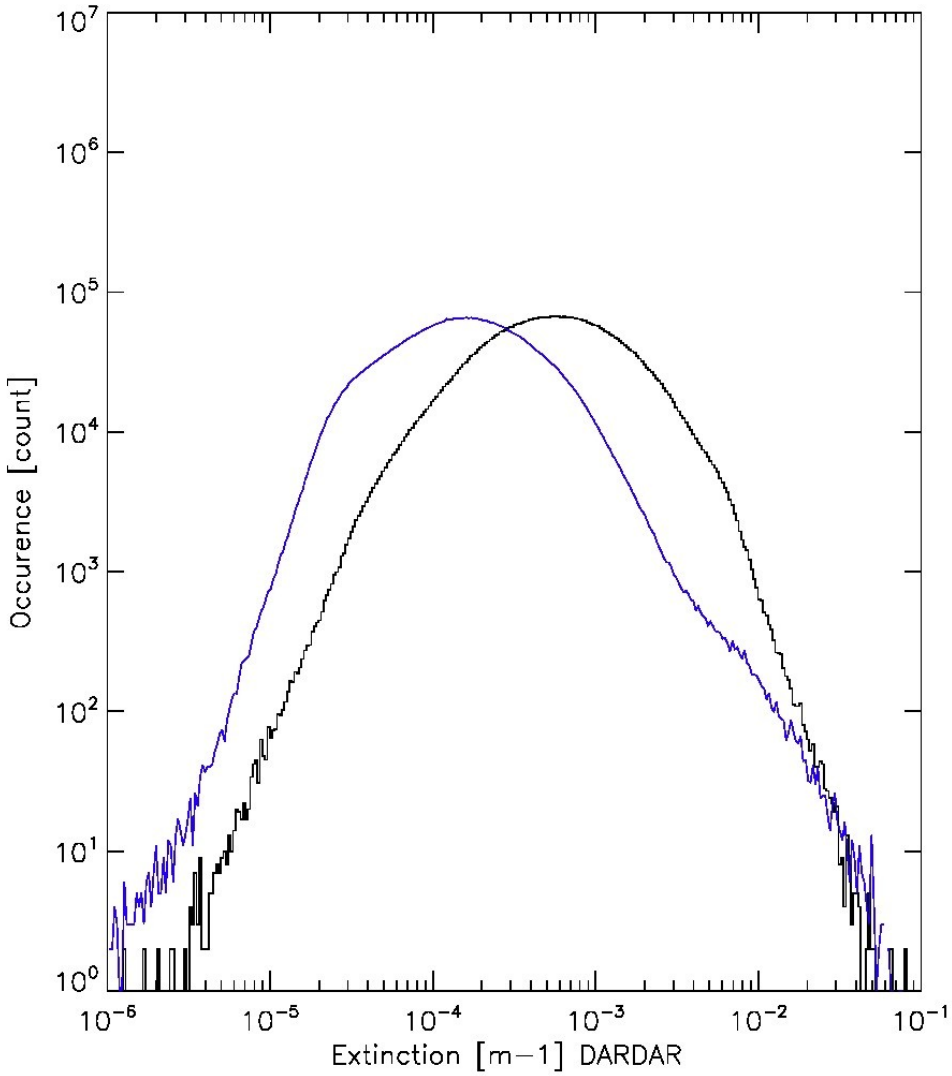

Figure 4: Histogram of the extinction as given by the Lidar + radar pixels (Black line), and by the lidar only pixels (Blue line).

From that extinction values, and using the temperature provided inside the same DARDAR-CLOUD product, we have been able to generate the values of the IWC using the parametrization given in section 5.5. Figure 5, shows the histogram corresponding for each of the classes **L+R** (Black line), **L** (Blue line). As the IWC grows, when the extinction grows, it is logical to retrieved lower value of IWC for the class (**L**) in comparison to ones given in the class (**L+R**). It can be said also here, that due to the fact that radar is less sensitive to lower extinction clouds than in the case of the lidar, it is also coherent that we find higher values of the IWC for the class (**R**).

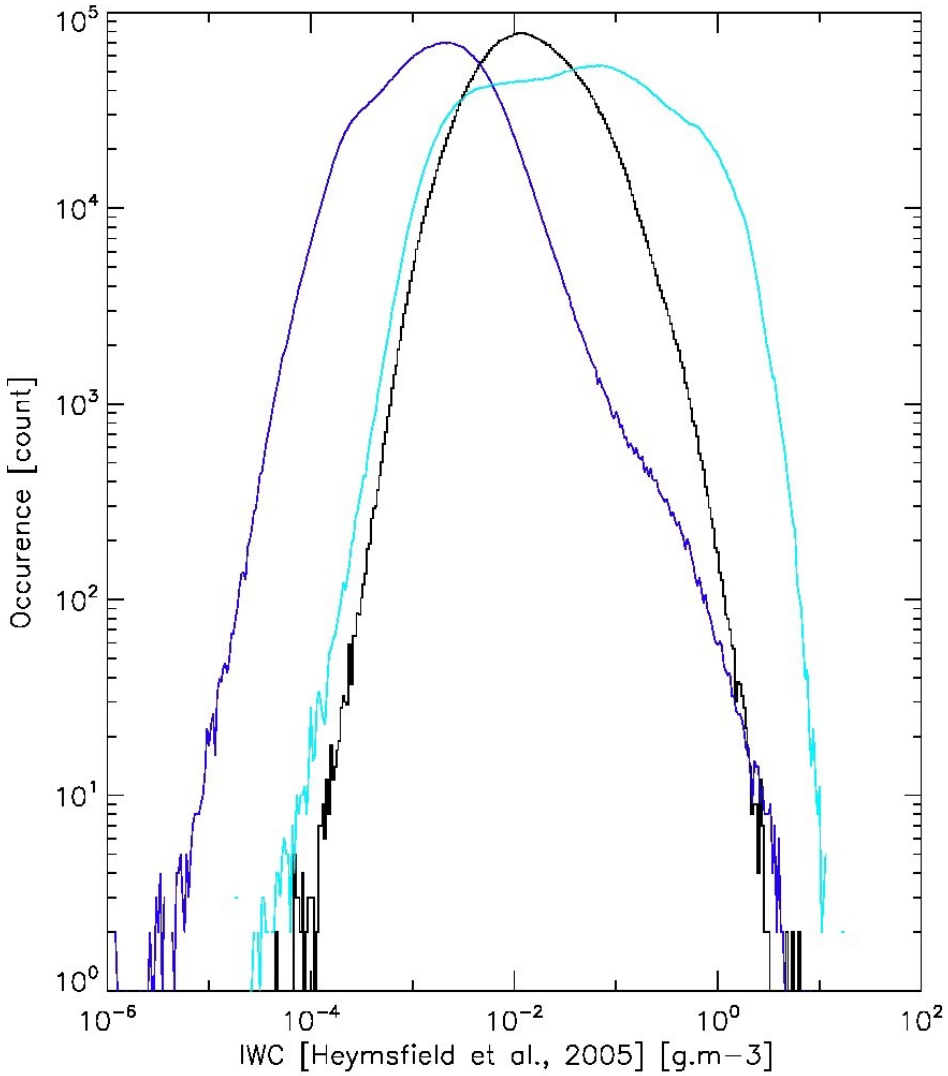

Figure 5: Histogram of the IWC as given by the Lidar + radar pixels (Black line), the lidar only pixels (Blue line), and the radar only pixels (cyan line)

Figure 6 presents the 2-D histogram of the extinction vs the IWC using values provided by the DARDAR product. The three different distribution seem to follow the same line. However, due to the different characteristics of lidar and radar instruments, the maximums of the occurrence of these distribution are not retrieved at the same [IWC, Extinction] values.

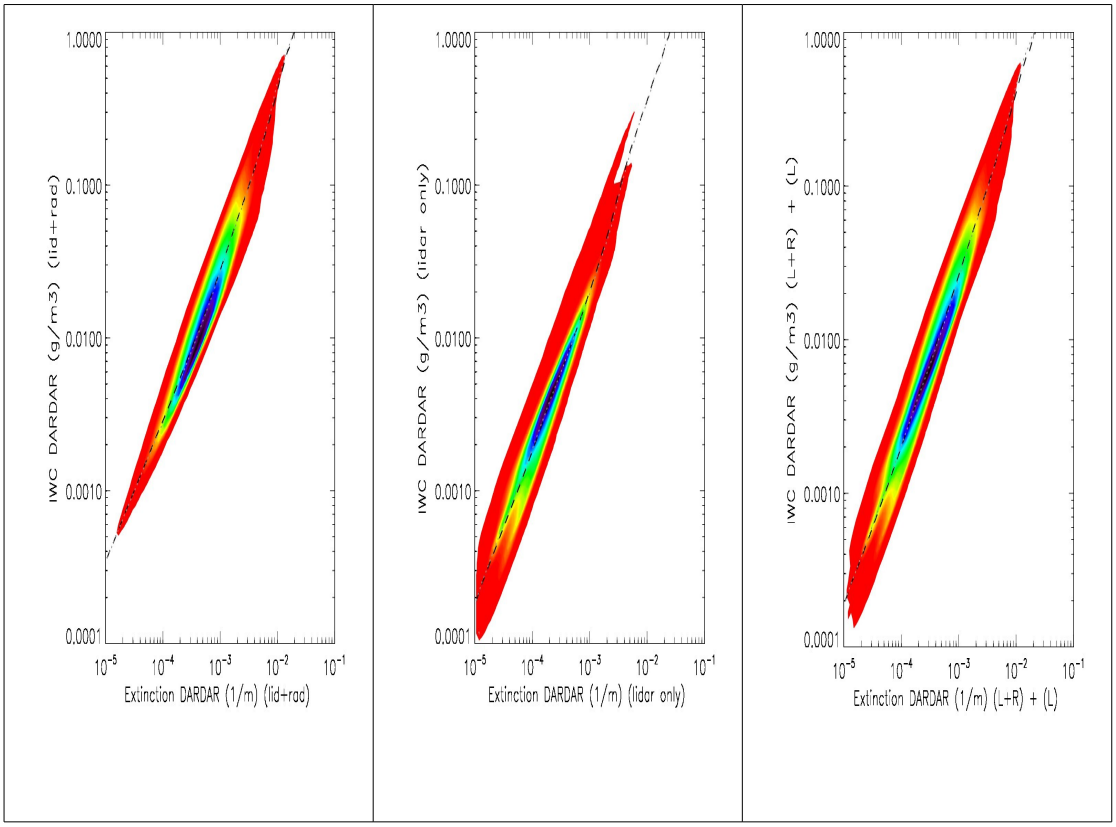

Figure 6: 2D-Histogram of the extinction vs IWC as given inside the DARDAR product. From left to right figure : (1) Lidar + Radar pixels, (2) Lidar only pixels. The last panel give the total (L+R) + (L) distribution.

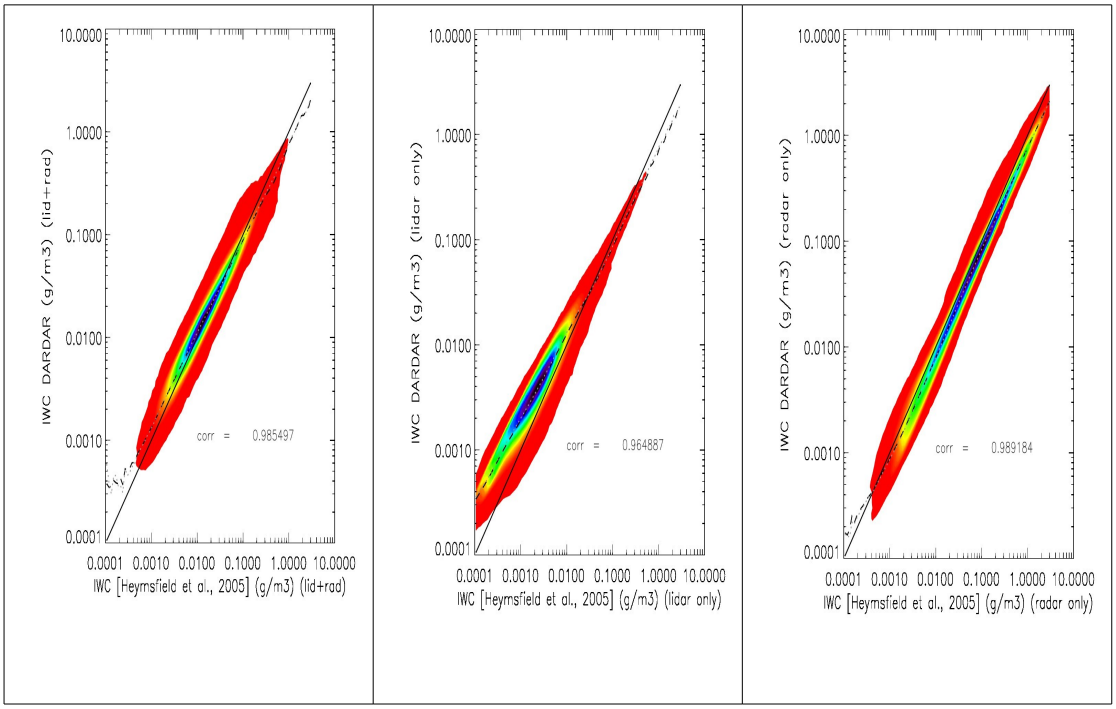

Figure 7: 2D-Histogram of correlation between IWC as given by the Heymsfield parametrization, against the product as given inside the DARDAR product : From left to right (1) Lidar + Radar pixels, (2) Lidar only pixels, (3) Radar only pixels.

To compare the IWC as retrieved by the [Heymsfield, 2005] method and one given by the DARDAR product, we proceed to the determination of the 2-D histogram of the correlation (see Figure 7). We retrieve strong correlation coefficients with 0.98 being obtained for the **(L+R)** class, and about 0.96 for lidar **(L)** class.

It must be noted here that for the panel representing the lidar only pixels, a kink appear inside the IWC correlation. This important point must checked in a future study.

To support the analysis of the characteristics of the sensitivities of the different instruments, we give in the figure 8, the dependence of the IWC/extinction ratio, in function of the temperature T. Figure 8 shows that, as lidar is more sensitive to high semi-transparent cloud, the statistics corresponding to this last class is more likely to be associated with lower temperatures (higher altitudes), in comparison to the (**L+R)** class.

NB : The **(R)** class is not given here as no radar measurement is made, and thus no reflectivity measurement are available.

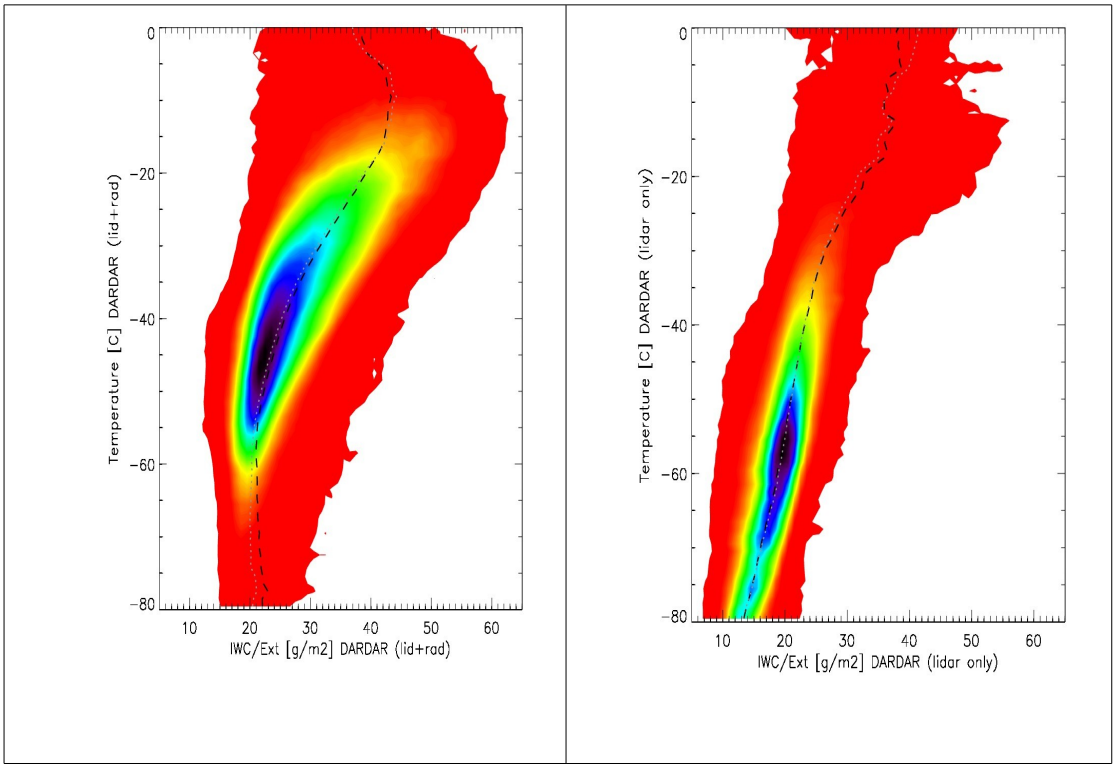

Figure 8: 2D-Histogram of the dependence of the IWC/extinction ratio in function of the temperature. From left to right : (1) Lidar + Radar pixels, (2) Lidar only pixels.

6.3. Reff retrieval : comparison with DARDAR result

Following the method described inside the [Foot, 1988] parameterization (see section 5.5.), we have been able to construct the histogram of Reff corresponding to **(R+L)** and **(L)** classes.

As this product is directly proportional to the IWC/Extinction ratio, the distribution corresponding to lidar class **(L)** is shifted to lower values of Reff in comparison to results given by **(L+R)** measurements.

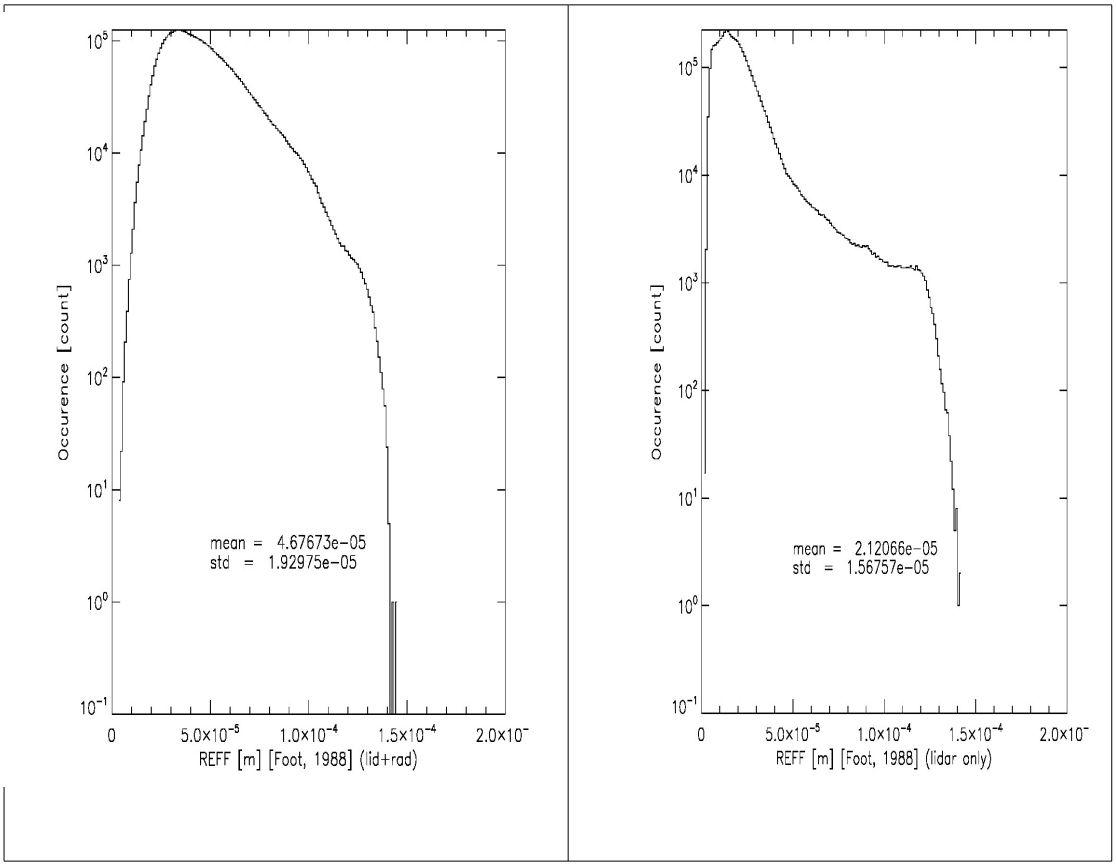

Figure 9: Histogram of the effective radius : from left to right, (1) Lidar + radar pixels (Black line), (2) the lidar only pixels.

The correlation between Reff as retrieved from the DARDAR-CLOUD product and that given after application of the Foot parametrization show differences (see Panels in Figure 10).

In particular, in the case of the **(L+R)** class, a strong correlation is retrieved.

To conclude this analysis unexpected behaviour of the correlation in the case of the **(L)** class was found. The distribution is very narrow, with a bias that occurs in comparison to the Foot method. This behaviour seem to be the representation of the use of a very strong parametrization within the DARDAR-CLOUD product. Indeed, the DARDAR-CLOUD product rely on a parametrization and archival informations, whereas our method only use one parametrization.

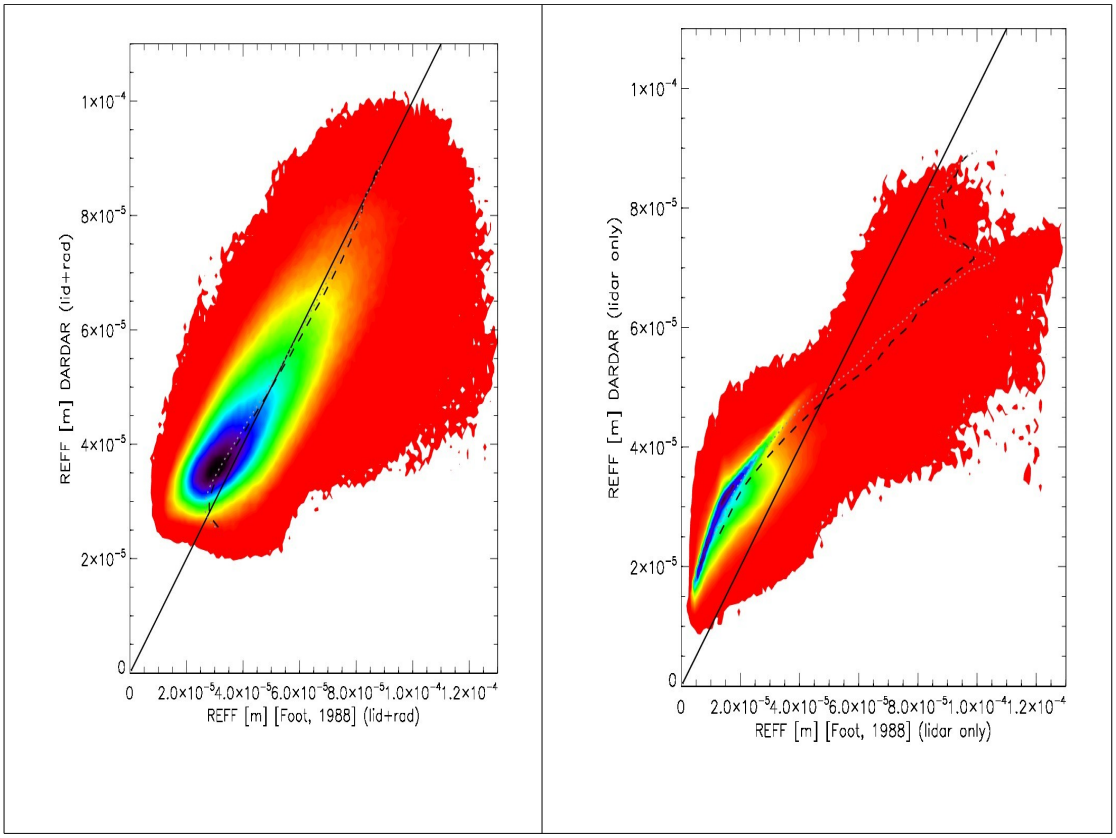

Figure 10: 2D-Histogram of correlation between the effective radius as given by the Foot [Foot, 1988] parametrization, against the product as given inside the DARDAR product : From left to right figure : (1) Lidar + Radar pixels, (2) Lidar only pixels.

7. Validation status

The prototype algorithm has been implemented as an IDL routine and is not integrated into the ECSIM environment. The application of the IWC-Extinction parameterization to the DARDAR extinction output shows that the resulting IWC values are largely consistent with the DARDAR existing IWC product. However, , at this point unexplained, inconstancies may be present for low reflectivity (low IWC) clouds.

8. Future validation needs

Some part of this algorithm need to be developed in the future :

- A full error assessment is needed in the retrieval for all the retrieved parameters.
- The evaluation of IWC and R_{eff} products will require comparisons with aircraft borne in-situ measurements.
- An Ice crystal type may be determined in the future. This work will likely evolve after the launch of the EarthCARE mission.